Bioactive Materials 6 (2021) 4377–4388

Contents lists available at ScienceDirect

Bioactive Materials

journal homepage: www.sciencedirect.com/journal/bioactive-materials

Sand-mediated ice seeding enables serum-free low-cryoprotectant cryopreservation of human induced pluripotent stem cells

Bin Jiang [a,1], Weijie Li [a,b,1,**], Samantha Stewart [a,1], Wenquan Ou [a], Baolin Liu [b], Pierre Comizzoli [c], Xiaoming He [a,d,e,*]

[a] Fischell Department of Bioengineering, University of Maryland, College Park, MD, 20742, USA
[b] Institute of Biothermal Technology, University of Shanghai for Science and Technology, Shanghai, 200093, China
[c] Smithsonian Conservation Biology Institute, National Zoological Park, Washington, DC, 20008, USA
[d] Robert E. Fischell Institute for Biomedical Devices, University of Maryland, College Park, MD, 20742, USA
[e] Marlene and Stewart Greenebaum Comprehensive Cancer Center, University of Maryland, Baltimore, MD, 21201, USA

ARTICLE INFO

Keywords:
Sand
Ice seeding
Cryopreservation
iPSC
Stem cell

ABSTRACT

Human induced pluripotent stem cells (hiPSCs) possess tremendous potential for tissue regeneration and banking hiPSCs by cryopreservation for their ready availability is crucial to their widespread use. However, contemporary methods for hiPSC cryopreservation are associated with both limited cell survival and high concentration of toxic cryoprotectants and/or serum. The latter may cause spontaneous differentiation and/or introduce xenogeneic factors, which may compromise the quality of hiPSCs. Here, sand from nature is discovered to be capable of seeding ice above −10 °C, which enables cryopreservation of hiPSCs with no serum, much-reduced cryoprotectant, and high cell survival. Furthermore, the cryopreserved hiPSCs retain high pluripotency and functions judged by their pluripotency marker expression, cell cycle analysis, and capability of differentiation into the three germ layers. This unique sand-mediated cryopreservation method may greatly facilitate the convenient and ready availability of high-quality hiPSCs and probably many other types of cells/tissues for the emerging cell-based translational medicine.

1. Introduction

Human induced pluripotent stem cells (hiPSCs), with their capacity of differentiating into all the three germ layers [1], have tremendous value for both research to understand human diseases and clinical application to treat the diseases [2,3]. For example, they have been explored for tissue engineering, disease modeling, and personalized medicine, which requires the ready availability of a large number of cells (up to billions) [2,4–6]. Therefore, effective long-term cryopreservation or banking of hiPSCs to maintain high viability, function, and pluripotency of the cells for their wide distribution and future use is necessary for the eventual success of the emerging stem cell-based medicine [7–10]. Conventional hiPSC cryopreservation uses a slow-freezing method in the presence of 10% dimethyl sulfoxide (DMSO) as the cryoprotectant (CPA) and 10% fetal bovine serum (FBS) or serum replacement. DMSO is effective at protecting the cells from injury during cryopreservation but is highly toxic to cells and tissues at body temperature [11–14]. Furthermore, DMSO has been found to induce differentiation in more than 25 human stem cell lines [15] and cause changes in the cellular processes and epigenetic landscape of cardiac cells [16]. The use of fetal bovine serum (FBS) for cryopreservation poses the risk of spontaneous differentiation and introduction of possible xenogeneic pathogens into the hiPSC sample, which may cause adverse effect to patients transplanted with the hiPSCs or their derivatives [17,18]. These risks underscore the need for better hiPSC cryopreservation protocols.

During slow-freezing of cells in aqueous samples, ice usually nucleates and grows in the extracellular space first [19–21]. However, uncontrolled spontaneous ice nucleation is a stochastic event that often occurs at temperatures below −10 °C [22], which may be detrimental

Peer review under responsibility of KeAi Communications Co., Ltd.
** Corresponding author. Current address: Institute of Biothermal Technology, University of Shanghai for Science and Technology, Shanghai, 200093, China.
* Corresponding author. Fischell Department of Bioengineering, University of Maryland, College Park, MD, 20742, USA.
E-mail addresses: liweijie10@139.com (W. Li), shawnhe@umd.edu (X. He).
[1] These authors contribute equally.

https://doi.org/10.1016/j.bioactmat.2021.04.025
Received 17 February 2021; Received in revised form 14 April 2021; Accepted 14 April 2021

and often lethal to cells [23–26]. This is because the lower the subzero temperature when ice nucleation occurs, the more ice embryos can be nucleated (and the finer ice crystals can be formed, due to the same amount of water available for ice embryos to grow in a given space) [22,26]. At a low subzero temperature like −10 °C or below, the fine ice crystals formed outside cells may easily pierce through the cell membrane to cause physical damage and induce the formation of fine ice crystals of intracellular water that is also deeply supercooled with high tendency of forming ice [23–26]. Intracellular ice formation (IIF) has been well-recognized to be a lethal event to cells in general [23–26]. In addition, the sudden/rapid ice formation at low subzero temperatures can cause a rapid increase in the local osmolality of the extracellular solution around the growing ice crystals, which might also induce osmotic shock-associated damage to cells [26]. In contrast, controlled ice nucleation at a high subzero temperature enables the nucleation of reduced number of ice embryos that gradually grow into large ice crystals outside cells with further cooling, which may allow enough time for intracellular water to gradually diffuse out of cells in response to the gradual freezing of extracellular water to minimize both IIF and osmotic shock [23–26]. This is crucial for cryopreserving stress-sensitive cells like embryos although the degree of its impact on the outcome of cryopreservation may be cell-type dependent [26,27].

A number of methods have been used to control ice nucleation in samples during cryopreservation to improve the outcome [27,28]. Early studies manually "seed" ice by introducing ice crystal into a supercooled sample [29]. Later, to reduce the risk for sample contamination, precooled probes, metal rods, or forceps have been used to create cold spots from the outside wall of the cell container (e.g., cryovial), thereby providing localized deep supercooling (usually below −20 °C) to induce ice nucleation in a sample that is above −10 °C overall [26,30]. However, manual ice seeding is difficult to standardize and lengthy because it often requires multiple trials to induce ice formation. To address these issues, ice nucleators including the bacterium *Pseudomonas syringae* [31–34], crystalline cholesterol [35], and silver iodide [36,37], have been added to the samples for inducing ice formation or seeding ice above −10 °C. However, these ice nucleators can be difficult to make in compliance with the current good manufacturing practice (cGMP) and/or are not biocompatible, and therefore may not be suitable for cryopreserving clinical grade stem cells [27].

Inspired by the phenomenon in nature that ice is usually observed next to the bank of rivers, lakes, and ponds at high subzero temperatures in the winter, we discovered that sand particles immobilized on a plastic surface can initiate ice nucleation consistently above −10 °C in this study. Based on this discovery, we further developed a simple and cost-effective method by utilizing sand to seed ice for cryopreservation. This enables serum-free cryopreservation of hiPSCs with high viability (90%), pluripotency, and function at a much-reduced cryoprotectant concentration (5%). Sand particles can be easily immobilized on the inner plastic surface of the cryovials for holding cells to prevent them from entering the cell sample, and they can be conveniently separated from cells because sand has much higher density than cells. These together with the non-toxic nature of sand may make the sand-mediated ice-seeding method very attractive for enhanced cryopreservation of hiPSCs and possibly many other types of cells for widespread research and clinical applications.

2. Materials and methods

2.1. Cell culture

The DF19-9-11T.H and IMR90-1 hiPSC lines were purchased from WiCell (Madison, WI, USA). The cells were cultured in StemFlex medium (ThermoFisher, Gaithersburg, MD, USA) on Matrigel (Corning, NY, USA)-coated plates in a 37 °C 5% CO_2 incubator. The cells were passaged at a ratio between 1:4 and 1:5 twice a week. Versene (Gibco, Gaithersburg, MD, USA) which contains 0.48 nM ethylenediaminetetraacetic acid (EDTA) in phosphate buffered saline (PBS) was used to detach the cells at 37 °C for 2 min for passaging or further uses.

2.2. Fabrication of sand-PDMS film for cryopreservation

Sands were purchased from Walmart (Landover Hills, MD, USA) and were rinsed under running tap water overnight in a 100-mL beaker (with agitation by a glass stir bar for 10 min at the beginning). The sand was then washed twice with 50 mL of deionized water. Afterwards, the sand samples were autoclaved at 121 °C for 30 min and baked in a 75 °C oven for 6 h to dry. Polydimethylsiloxane (PDMS, Dow SYLGARD 184 Silicone Encapsulant, Dow, Midland, MI, USA) prepolymer was mixed with its curing agent at a weight ratio of 10: 0.5 (prepolymer: curing agent). The mixture (1 mL) was poured onto a microscope glass slide (75 × 26 × 1 mm) and air bubbles were removed under vacuum for 20 min. Afterwards, the PDMS was cured by baking in a 75 °C oven for 2 h. Uncured PDMS mixture (50 μL) was then evenly spread with the aid of a pipette tip on top of the cured PDMS on the glass slide to form a sticky fluid layer. Afterwards, the dry sands were sifted through a mesh strainer (opening size: 200 μm) at ~5 cm above to drop and partially embed the sands in the uncured PDMS sticky fluid layer. The slide with PDMS and sand was further baked in the oven at 75 °C for 30 min. The cured sand-PDMS film was gently peeled off from the slide with the help of a blade and then cut into pieces of 3 mm × 5 mm (width x length). Finally, each of the sand-PDMS pieces was attached to the inside wall of a cryovial and the sand-PDMS piece containing cryovials were autoclaved at 121 °C for 30 min before their use to hold hiPSC sample for cryopreservation.

For making the plastic shard-PDMS film, plastic shards were scratched off a polystyrene cell culture plate (ThermoFisher) using a single edge razor blade onto the uncured PDMS sticky layer (with all other steps being the same as that for making the sand-PDMS film). Glass beads of 40–70 μm in size were purchased from Microspheres-Nanopheres (C-PGL-07, Microspheres-Nanospheres, NY, USA). The glass beads were partially embedded in the PDMS film following the same procedure for making sand-PDMS film.

2.3. Surface characterization of the sand-PDMS film

For the scanning electron microscopy (SEM) imaging, the sand-PDMS films were cut into small pieces of 1 cm^2 and attached on the SEM sample holder. The samples were sputter-coated with gold using a Cressington (Watford, UK) 108 sputter coater for 2 min at 15 mA. Afterwards, the samples were imaged with a Hitachi (Tokyo, Japan) SU-70 FEG scanning electron microscope at 5.0 kV. Energy dispersive x-ray spectroscopy (EDXS, Hitachi SU-70 FEG SEM, Tokyo, Japan) was used for elemental analysis of the surface of the plain PDMS and sand-PDMS films. The plain PDMS film was prepared in the same way as that for preparing the sand-PDMS films except that no sand was plated.

For quantifying the size of sand particles before and after sifting, brightfield microscopy images of sand particles partially embedded in the PDMS film without and with sifting through the mesh strainer were analyzed using Image J (version 1.47) to measure the area of sand particles on the film. Images from 10 random areas of the film containing a total of 65 sand particles were analyzed for both conditions (i.e., without and with sifting through the mesh strainer).

2.4. Measurement of ice-seeding temperature

To measure the ice-seeding temperature, a piece of sand-PDMS film was attached to the inside wall of a 2-mL glass vial, followed by adding 500 μl of deionized water. The ice-seeding temperatures of water in the same glass vials containing either a PDMS-film without sand or no film at all were studied as controls. A K-type thermocouple (Omega, Norwalk, CT, USA, 0.05 inch in diameter) was then placed in water in the glass vial. The vials were placed onto the shelf of a SP Virtis AdVantage Pro benchtop lyophilizer (SP, Warminster, PA, USA) and cooled to 4 °C.

Then the sample was cooled to −25 °C with a 25-min ramp time. The thermocouple was connected to a Keysight Technologies (Santa Rosa, CA, USA) 34970A Data Acquisition/Data Logger Switch Unit to record the temperature over time. The temperature at the time when there was a sudden increase in temperature due to the latent heat release associated with ice formation during the cooling process, was recorded as the ice-seeding temperature. Ice-seeding temperatures of the plastic shard- and glass bead-PDMS films were measured in the same way.

2.5. Cryomicroscopy study of sand-mediated ice formation

Cryomicroscopy was conducted using a Linkam FDCS196 (Tadworth, UK) freeze-drying stage mounted on a Zeiss (Oberkochen, Germany) A1 Axio Scope, for which a drop (200 μL) of the cryopreservation solution made of the mTeSR medium (STEMCELL Technologies, Vancouver, Canada) supplemented with 5% DMSO, and sands were added in the sample holder at room temperature. The sample holder with the sands immersed in the solution was then loaded into the freeze-drying stage for controlled cooling at 1 °C min^{-1} to −20 °C. Real-time images were captured with a FLIR (Wilsonville, OR, USA) Grasshopper 3 color camera every 0.5 s.

2.6. Cell cryopreservation

The cryopreservation of hiPSCs was performed using a slow-freezing procedure with a Mr. Frosty™ Freezing Container filled with isopropyl alcohol (Sigma Aldrich), which has a cooling rate of approximately −1 °C min^{-1} [26,38]. The hiPSCs at 80% confluence were detached using Versene and suspended in pre-cooled cryopreservation solution. For the conventional method, the cryopreservation solution was made up of 10% FBS and 10% DMSO in the mTeSR medium. For the experimental cryopreservation solution, it contained 0–5% DMSO in the mTeSR medium with no FBS. All cryopreservation solutions and the Mr. Frosty™ Freezing Container were pre-cooled at 4 °C for 30 min before use. The concentration of hiPSCs for cryopreservation was 1×10^7 cells mL^{-1} and each cryovial was loaded with 250 μL of the cell suspension. Experimental conditions with sand-mediated ice seeding had one sand-PDMS film attached to the inside wall of the cryovial, with the sand surface being exposed to the cell suspension. The cryovials were loaded in the Mr. Frosty™ Freezing Container and stored in a −80 °C refrigerator overnight. Then, the cryovials with hiPSCs were transferred into the liquid nitrogen for long-term storage (2–5 weeks).

To thaw the frozen samples with hiPSCs, 2 mL of mTeSR medium with 10 μM ROCK inhibitor (RI, Y-27632, Sigma Aldrich) was added to each well (Matrigel coated) of a 6-well plate and pre-warmed in the incubator at 37 °C for at least 20 min. The cryovial was removed from the liquid nitrogen tank and rapidly warmed in a 37 °C water bath for ~30 s. The cell suspension in the cryovial was then transferred into the pre-warmed medium in the 6-well plate for further incubation and studies. DMSO was not removed immediately after thawing to avoid centrifuging and washing the hiPSCs. The cells were cultured in the 6-well plate with medium containing a final DMSO concentration of 0.56% (250 μL cell suspension containing 5% DMSO diluted in 2 mL medium). After 2 h, the DMSO-containing medium was replaced with pre-warmed DMSO-free medium.

2.7. Live/dead assay and cell attachment efficiency

To quantify their viability, the hiPSCs after thawing were cultured for 2 h and then stained with calcein AM and propidium iodide (PI) to visualize live (green with no red stain) and dead (red stain) cells, respectively, according to the instructions of the manufacturer (ThermoFisher). The two dyes were added into 1 mL of DMEM/F12 (1 μM for calcein AM and 1 μg mL^{-1} for PI) for incubating with the cells for 5 min at 37 °C. Afterwards, green and red fluorescence images of the samples were taken using a Zeiss (Oberkochen, Germany) LSM710 microscope to count the live and dead cells. Cell viability is calculated as the percentage of live cells out of the total (i.e., live and dead) cells.

To quantify the cell attachment efficiency for studying the capability of the hiPSCs in attaching on culture dish, the mTeSR medium containing ROCK inhibitor was replaced with fresh mTeSR without ROCK inhibitor after 2 h of post-thawing incubation. After 15 h of culture, the hiPSCs were detached and the cell number was counted. The cell attachment efficiency was calculated as the percentage of the cell number post-cryopreservation and 15 h of culture out of the cell number used for cryopreservation in the cryovial.

2.8. Teratoma assay

For the teratoma assay, hiPSCs at a confluence of 80% were detached and suspended at 3×10^7 cells mL^{-1} in 1 mL of 1x PBS and then mixed with 500 μL of Matrigel (Corning). The cell suspension was kept on ice and then injected subcutaneously (s.c.) into the dorsal rear flank of non-obese diabetic/severe combined immunodeficiency mice (NOD.CB17-scid, Charles River, Frederick, MD, USA). Each mouse was injected with 250 μL of the cell suspension and 5 mice (age: 5 weeks) were used for each experimental group. After 5 weeks, the mice were sacrificed and teratomas ($n = 5$ for each group) were collected. The samples were fixed in 4% paraformaldehyde (PFA) in 1 x PBS for 2 days. Afterwards, the samples were trimmed and embedded in paraffin for sectioning into slices of 5 μm in thickness. The slices were than stained with hematoxylin and eosin (H&E) and imaged with a Zeiss LSM710 microscope. All animal studies were approved by the Institutional Animal Care and Use Committee (IACUC) at the University of Maryland, College Park, MD.

2.9. Neural and cardiac differentiation

Neural differentiation was carried out by following previously reported studies [39–41]. Briefly, the hiPSCs were detached and suspended in mTeSR medium at 1×10^6 cells mL^{-1}. The samples were passed through a 70 μm cell strainer (Gibco). The resultant hiPSC samples were cultured in mTeSR with 10 μM ROCK inhibitor (Y-27632) for 2 days. Afterwards, the medium was replaced with a neural differentiation medium and the cells were further cultured for 10 days with medium being changed every other day. The neural differentiation medium was a mixture of DMEM/F12 and neural basal medium (Gibco) (1:1 in volume) supplemented with 1x N2 (Gibco), 1x B27 (Gibco), 1% minimum essential medium non-essential amino acids (MEM NEAA, Gibco), and 1% L-glutamine (Invitrogen, Carlsbad, CA, USA). Lastly, the cells on day 10 post-initiation of neural differentiation were fixed with 4% PFA for further immunostaining and analysis.

Cardiac differentiation was conducted also by following previous studies [42,43]. The basal medium used for cardiac differentiation was a mixture of DMEM/F12 and α-MEM (ThermoFisher) (1:1 in volume) supplemented with 2% Knockout Serum Replacement (KOSR, Gibco), 1 mM L-glutamine, 1% MEM NEAA, and 0.1 mM β-mercaptoethanol (Sigma Aldrich). For cardiac differentiation, hiPSCs were grown in 6-well plate coated with Matrigel. At 80% confluency, the hiPSCs were cultured with the mesoderm induction medium for 2 days. Then, the medium was replaced with the cardiac induction medium for the following 8 days. Medium change was performed every other day. The mesoderm induction medium was made by supplementing 5 μM CHIR99021 (ThermoFisher) and 2 μM GSK inhibitor 6-bromoindirubin-3′-oxime (BIO, ThermoFisher) in the basal medium. The cardiac induction medium was made by supplementing 10 μM KY02111 (ThermoFisher) and 10 μM XAV939 (ThermoFisher in the basal medium. Spontaneous beating areas in the sample were recorded using a Zeiss LSM710 microscope. The cells on day 10 post cardiac differentiation were fixed with 4% PFA for further immunostaining and analysis.

2.10. Immunofluorescence staining

For immunofluorescence staining, cells fixed with 4% PFA were gently rinsed twice with 1x PBS to remove the PFA, permeabilized with 0.1% TritonX-100 (Sigma Aldrich) in saline for 10 min, incubated with 0.1% Tween-20 (Sigma Aldrich) and 5% normal goat serum (Invitrogen) in saline for 2 h at room temperature (RT) to block non-specific binding. Afterwards, the samples were incubated with primary antibodies at 4 °C overnight. The primary antibodies and their respective dilutions were as follows: for pluripotency, OCT-4 (1:500 dilution, Cell Signaling Technologies, Danvers, MA, USA) and SSEA-4 (1:500 dilution, Cell Signaling Technologies); for cardiac differentiation, cTnT (1:500 dilution, Cell Signaling Technologies); for neural differentiation, TUJ-1 (1:500; R&D Systems, Minneapolis, MN, USA). The secondary antibodies (goat anti-rabbit IgG FITC and goat-anti-mouse IgG PE, Invitrogen) at 1:1000 dilution was incubated with the samples for 1.5 h at RT. Finally, the samples were rinsed with 1x PBS thrice and the nuclei were stained with DAPI (1 μg mL^{-1} in 1x PBS, Sigma Aldrich) for 5 min at RT before imaging with a Zeiss LSM710 microscope.

2.11. Flow cytometry analysis of protein marker expression

For flow cytometry studies of protein marker expression, cells were dissociated into single cells by incubating them with 0.25% trypsin (Gibco) for 5 min at 37 °C and washed with 1x PBS twice. The dissociated cells were fixed with 75% ethanol at 4 °C overnight. Then, the cells were permeabilized with 0.05% Triton X-100 for 3 min and rinsed with 1x PBS twice. The cell number was adjusted to 1×10^6 cells per tube in 700 μL of 1x PBS for each protein marker. The cells were incubated with primary antibodies including: OCT-4 (1:500 dilution, Cell Signaling Technologies), SSEA-4 (1:500 dilution, Cell Signaling Technologies), TUJ-1 (1:500; R&D Systems, Minneapolis, MN, USA), or cTnT (1:500 dilution, Cell Signaling Technologies) at 4 °C overnight. Afterwards, the samples were rinsed with 1x PBS thrice before incubation with secondary antibodies (goat anti-mouse IgG FITC and goat anti-rabbit IgG PE, Invitrogen) at 1:1000 dilution for 1 h at RT. The samples were then washed with 1x PBS twice before analysis using a BD FACSCelesta (Franklin Lakes, NJ, USA) flow cytometer. The cells incubated with secondary antibody but no primary antibodies were processed and washed in the same way for analysis to serve as the negative/isotype control. The resultant data was analyzed with the BD Flowjo software (v10).

2.12. Cell cycle analysis

For cell cycle analysis, the cells fixed as aforementioned for protein marker expression studies were treated with RNase from bovine pancreas (1 μg mL^{-1}, ThermoFisher) for 5 min at RT. Then, the cells were stained with PI (1 μg mL^{-1}, ThermoFisher) for 5 min at RT and rinsed with 1x PBS twice. Afterwards, the cell concentration was adjusted to 1×10^6 cells per tube in 700 μL of 1x PBS for analysis using a BD FACSCelesta flow cytometer. The resultant data was analyzed with the built-in cell cycle analysis function of the BD Flowjo software (v10).

2.13. Statistical data analysis

At least three independent runs on different days were conducted for each experiment. All quantitative data were analyzed with Graphpad Prism (version 8, San Diego, CA, USA) and presented as mean ± standard deviation. Student's t-test (two-tailed, unpaired, and assuming equal variance) was performed to assess the statistical significance of difference between two groups, and a difference with a p value less than 0.05 was considered to be statistically significant.

3. Results

3.1. Fabrication and characterization of sand-PDMS film

As illustrated in Fig. 1a and Fig. S1, sand-PDMS films were prepared for sticking on the inside wall in cryovials to seed ice and enhance the outcome of cryopreservation. The raw sands after cleaning (with water) and drying were gently sifted onto and partially embedded in a thin layer of uncured PDMS on top of a fully cured PDMS film using a mesh strainer with openings of 200 μm. After baking at 75 °C for 30 min to crosslink the uncured PDMS, the resultant sand-PDMS films are cut into small pieces (3 mm × 5 mm) and each piece is stuck via its smooth surface onto the inner wall of a cryovial for cryopreservation. The sand-PDMS film is soft and can be easily deformed onto the shape of the inner wall of cryovial for attaching to the wall via its smooth surface without any sand. No sands are observed to detach from the film when using the cryovial attached with the sand-PDMS film for cryopreservation studies, probably because the sands are partially embedded in the top PDMS layer to prevent them from detaching.

The sands are heterogeneous in size in nature (Fig. 1B, before sifting). After sifting with a 200 μm mesh strainer, the size of the resultant sand particles partially embedded in the PDMS film is significantly more homogenous than that before sifting and their sharp morphology is appreciable in the high-magnification image (Fig. 1B). Scanning electron microscopy (SEM) imaging of the sand-PDMS film shows that the sand protrudes out of the surface of the film, which is not seen on the plain PDMS surface (Fig. 1C). This is further confirmed by the energy dispersive X-ray spectroscopy (EDXS) data showing the higher occurrence of Silicon (Si) in the sand-PDMS film than the pure PDMS film (Fig. 1D–E), because the natural sand is made of silicon dioxide. This exposed sand may serve to nucleate/seed ice in the cryopreservation solution outside cells during cooling, similarly to that observed near river/lake/pond bank in nature.

3.2. Ice seeding with sand-PDMS film

The effect of sand on the ice-seeding temperature of water is investigated by measuring the change in temperature over time during cooling. Ice seeding in the sample can be detected by a sudden temperature rise (Fig. 2A), due to the release of latent heat of fusion as a result of ice nucleation and growth. Therefore, the temperature at which the sudden increase occurs is taken as the ice-seeding temperature. As shown in Fig. 2B, the ice-seeding temperature of water without any film (control) is −15.9 ± 1.6 °C. The addition of a pure PDMS film containing no sand in the cryovial causes no significant change in the ice-seeding temperature (−14.9 ± 2.0 °C). Importantly, when the sand-PDMS film is added into the cryovial, the ice-seeding temperature increases significantly to −7.8 ± 1.6 °C.

This capability of sands in seeding ice at the high subzero temperature is confirmed by cryomicroscopy studies to cool cryopreservation solution (mTeSR medium containing 5% DMSO) at −1 °C min^{-1}, as shown in Fig. 2C and Movie S1. Initially, there is no evident ice formation at −9.2 °C in the cryopreservation solution (Fig. 2C and 0 s) since the solution around or away from the sand is transparent (the slightly darker appearance near the sand is probably due to the light-shadowing effect of the sand). After 0.5 s, the solution next to the sand becomes darkened (indicated by the white arrow) compared to the solution away from the sand, indicating the sand induces ice formation in the solution. Growth of ice into the solution away from the sand can be seen at 1.5 and 10 s (one of the ice growth fronts is indicated by a white arrow in the image for each of the two times), during which the temperature decreases from −9.2 to −9.4 °C. This capability of sands in seeding ice in cryopreservation solution at a high subzero temperature may be useful for improving the outcome of cell cryopreservation, which is tested using hiPSCs.

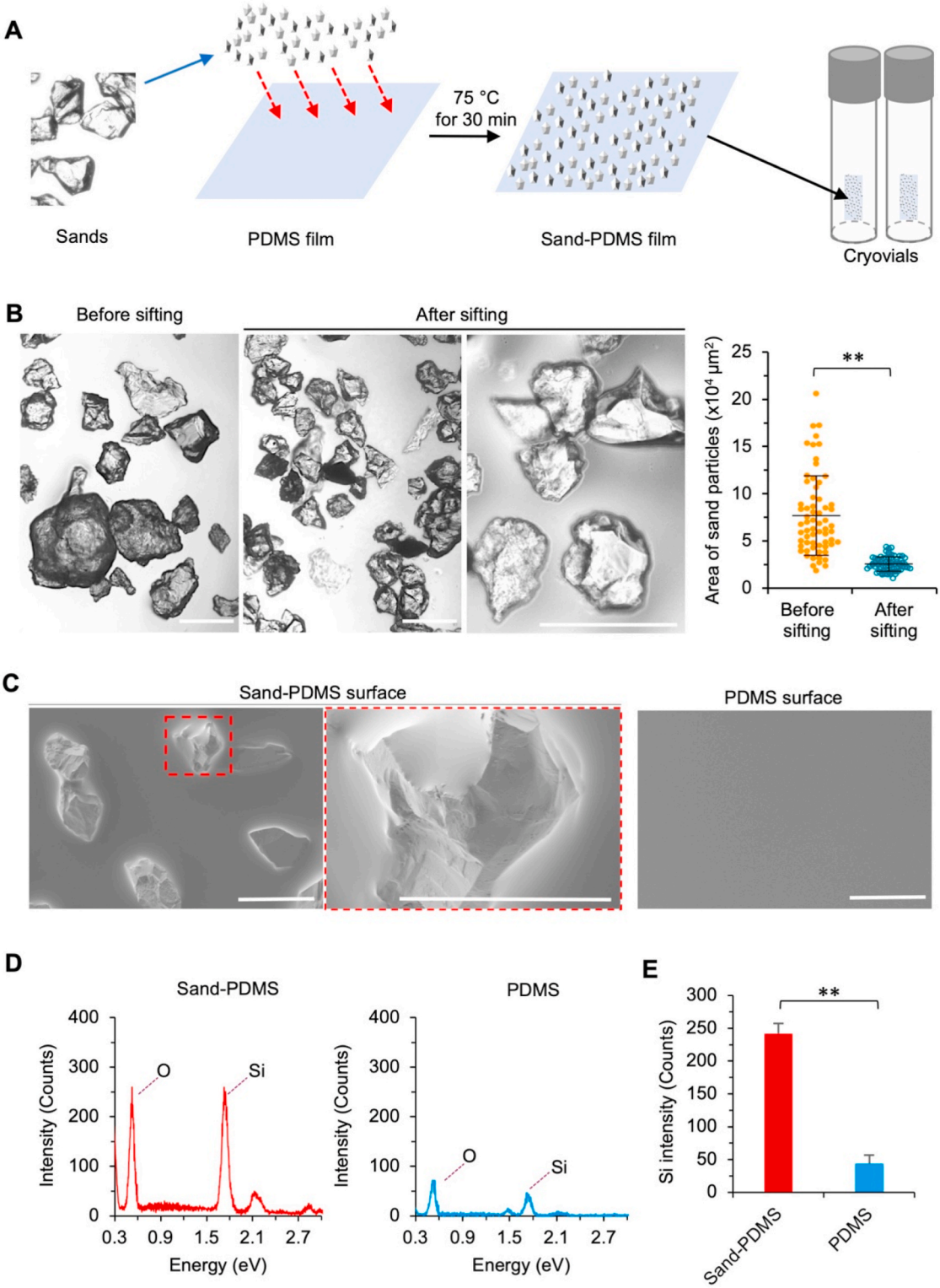

Fig. 1. Preparation and characterization of sand-PDMS film. (A) A schematic illustration of the procedure for preparing the sand-PDMS film: The sand was first rinsed overnight with water, autoclaved, dried, and then sifted onto a thin and uncured PDMS layer over a fully cured PDMS film through a mesh strainer with 200 μm openings. The PDMS film embedded with sand was baked at 75 °C for 30 min to form the sand-PDMS film. The sand-PDMS film was cut into small pieces and each piece was stuck/attached onto the inner wall of a cryovial via its smooth face. (B) Morphology and size distribution of sands before and after sifting them through the mesh strainer. Also shown is a high-magnification view of the sifted sands where the sharp morphology of the sands is more appreciable. The size distribution was quantified based on the area of sand particles on the films. (C) Scanning electron microscopy (SEM) image, showing the presence and morphology of sands partially embedded in the PDMS film. (D) Energy dispersive X-ray spectroscopy (EDXS) quantification of the elemental composition of the sand-PDMS and pure PDMS films. The surface of the sand-PDMS film contains an increased amount of silicon (Si) and oxygen (O) than the pure PDMS surface. (E) Quantification of Si counts for the sand-PDMS and pure PDMS films using EDXS. Scale bars: 200 μm **, $p < 0.01$ ($n = 3$ independent runs).

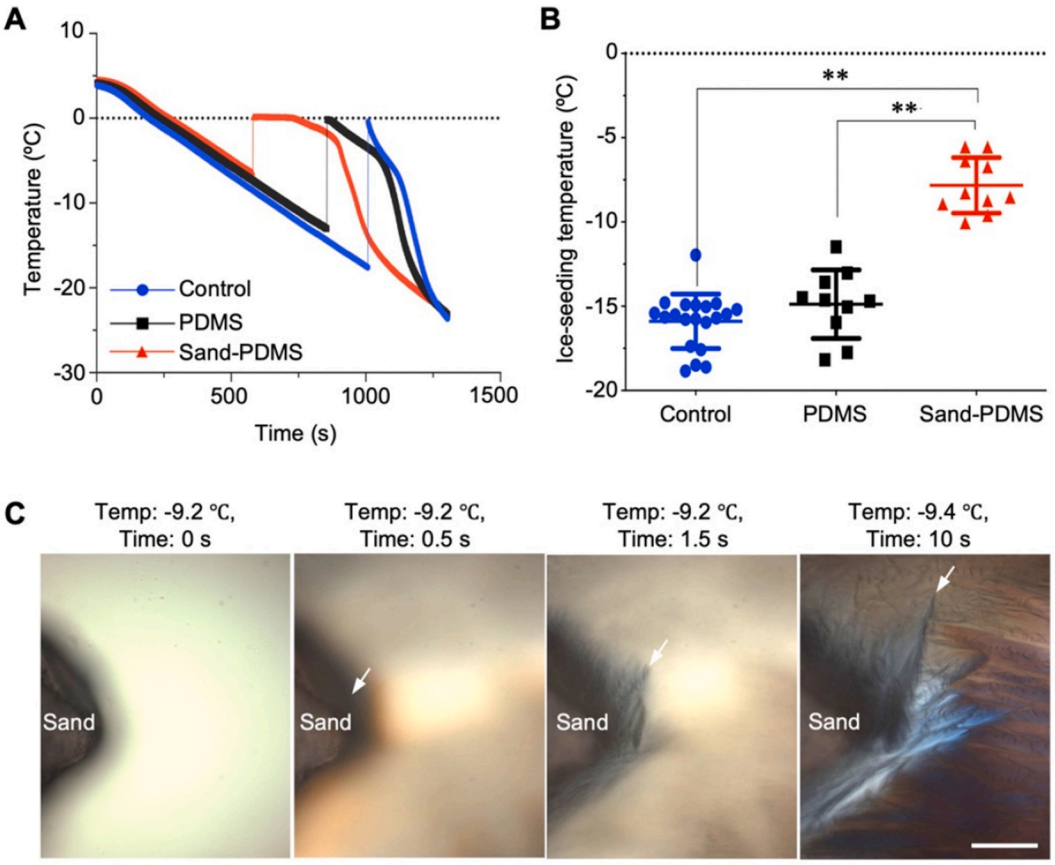

Fig. 2. Sand enables ice seeding at high subzero temperature. (A) Representative thermal histories in water containing no film (Control), pure PDMS film (PDMS), and sand-PDMS film (Sand-PDMS) during cooling. A sudden increase in temperature indicates ice seeding (which releases latent heat) in the sample. (B) Quantitative data of the ice-seeding temperature in water under the aforementioned three conditions. **, $p < 0.01$ ($n = 10$ (for sand-PDMS film and pure PDMS film) or 20 (for Control), independent runs). (C) Cryomicroscopy images at different times showing ice nucleation and growth around the sand particle during cooling the cell cryopreservation solution at subzero temperatures. Scale bar: 100 μm.

3.3. Enhanced cryopreservation of hiPSCs with sand-mediated ice seeding

To demonstrate the benefit of sand-mediated ice seeding for cryopreservation, hiPSCs are cryopreserved by slow-freezing under various conditions with or without the sand-mediated (by default) ice seeding: conventional method (10% DMSO and 10% FBS with no ice seeding), ice seeding alone, no cryoprotectant and no ice seeding, 5% DMSO and no ice seeding, 2% DMSO and ice seeding, and 5% DMSO and ice seeding. Fig. 3A shows typical live/dead (green/red) images of the hiPSCs cryopreserved under the various conditions and cultured for 2 h at 37 °C after thawing, and the corresponding quantitative data of cell viability are shown in Fig. 3B. Without the use of any cryoprotectant, the sand-mediated ice seeding alone is insufficient to protect the cells from injury during the cryopreservation procedure, as indicated by the low cell viability under this condition (5.6 ± 2.1%) that is only slightly higher than that for the condition with no cryoprotectant and no ice-seeding (1.3 ± 0.6%). The use of 2% DMSO together with the sand-mediated ice seeding could improve the hiPSC viability to 37.3 ± 3.1%, showing the importance of using cryoprotectant to reduce cryoinjury to the cells. The cell viability is further improved albeit still modest for both the condition of 5% DMSO with no ice seeding (52.6 ± 3.5%) and the conventional method using 10% DMSO and 10% FBS (51.7 ± 4.0%). This demonstrates 5–10% DMSO could only protect up to ~50% hiPSCs from cryoinjury during cryopreservation and increasing DMSO from 5% to 10% does not significantly enhance the hiPSC viability in the absence of ice seeding. Importantly, high viability (90.3 ± 2.5%) of the hiPSCs after cryopreservation can be achieved by combining the sand-mediated ice seeding with 5% DMSO. This viability is significantly higher than that of all the other control groups.

Because the aforementioned immediate (2 h) cell viability judged by the live/dead (green/red) staining assay is mainly a reflection of the cell membrane integrity, we further evaluate the cell viability (i.e., attachment efficiency) by determining the percentage of cells that can attach after culturing for 15 h post-thawing. Fig. S2 shows typical images of the cells after culturing for 15 h post-thawing, and the corresponding quantitative data are shown in Fig. 3B. Overall, the hiPSC attachment efficiency is slightly lower than the cell viability assessed based on membrane integrity for all the conditions, suggesting some cells with good membrane integrity judged by the live/dead assay may not be able to attach and survive in long term. Furthermore, the hiPSC attachment efficiency follows the same trend as the immediate cell viability for the various conditions, and it is significantly and greatly higher for the condition of 5% DMSO and ice seeding than all the other control conditions.

Taken together, both the immediate (2 h) cell viability and long-term (15 h) cell viability (i.e., attachment efficiency) data show that 5% DMSO is critical but further increasing DMSO may not be sufficient to protect hiPSCs from cryoinjury during cryopreservation, which can be resolved by combining 5% DMSO with the sand-mediated ice seeding to significantly and greatly enhance the outcome of hiPSC cryopreservation. Therefore, the hiPSCs cryopreserved by 5% DMSO and the sand-mediated ice seeding are further analyzed in terms of their pluripotency, cell cycle, and capability of differentiation to ascertain their long-term functional survival.

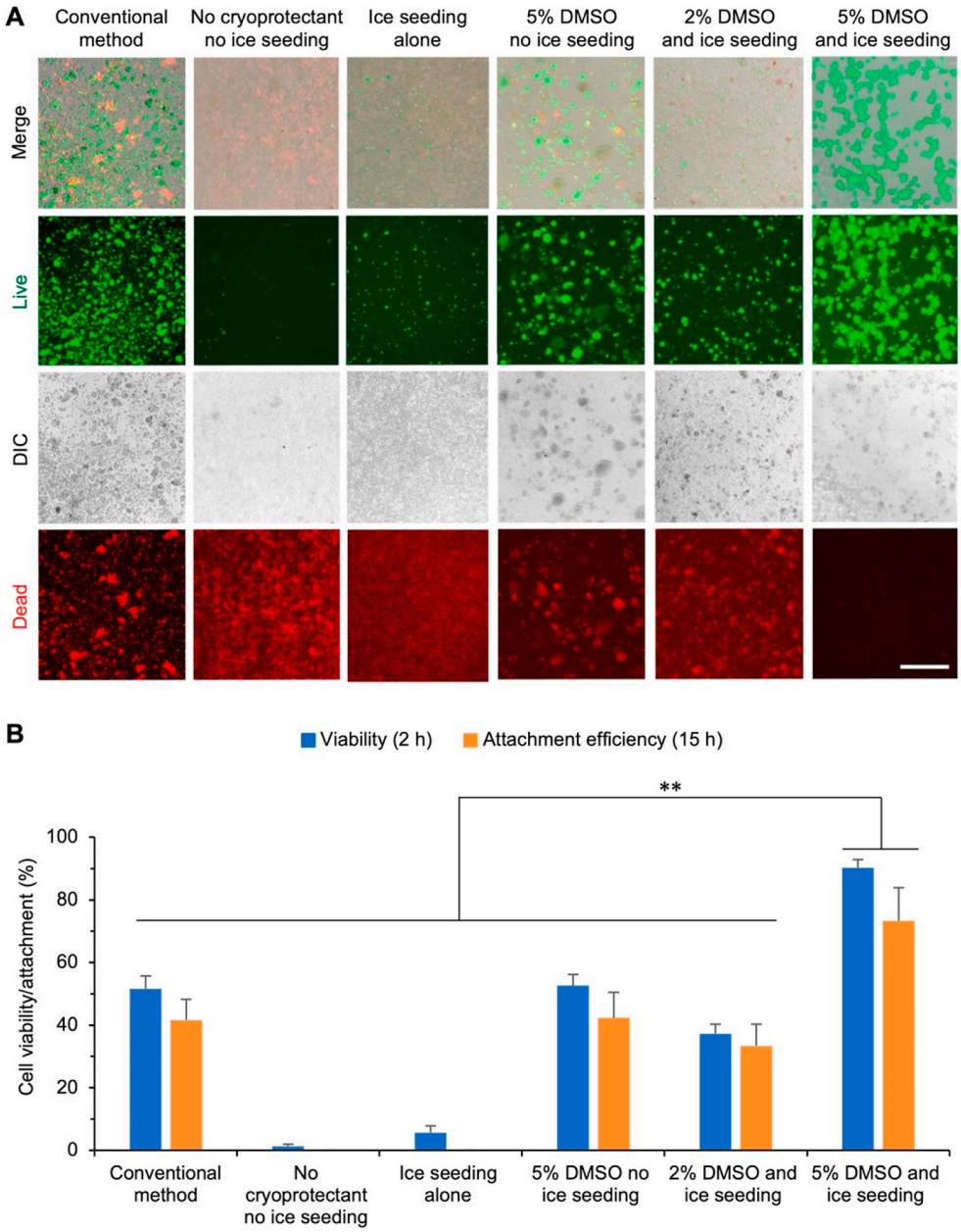

Fig. 3. The immediate and long-term viability of hiPSCs after cryopreservation under various conditions. (A) Immediate (after 2 h incubation at 37 °C) viability of hiPSCs assessed by live/dead (green/red) staining after cryopreservation with different methods: conventional method (10% DMSO+10% serum with no ice seeding), sand-mediated ice seeding alone, no cryoprotectant and no ice seeding, 5% DMSO with no ice seeding, 2% DMSO with ice seeding, and 5% DMSO with ice seeding. Scale bar: 500 μm. (B) Quantitative data of the hiPSC immediate viability and attachment efficiency (i.e., long-term viability) after the various cryopreservation conditions. For quantifying the attachment efficiency, the cryopreserved cells were thawed and cultured for 15 h, and the number of attached cells was counted by hemacytometer. The attachment efficiency is calculated as the percentage of cells counted after cryopreservation out of the number of cells initially cryopreserved. **, $p < 0.01$ ($n = 3$ independent runs) for the comparison of both immediate viability and attachment efficiency.

3.4. High pluripotency and normal cell cycle of cryopreserved hiPSCs

The hiPSCs cryopreserved (cryo) using 5% DMSO and the sand-mediated ice seeding show typical colony morphology similar to that of fresh (control) hiPSCs under 2D monolayer culture (Fig. 4A). Furthermore, the cryopreserved hiPSCs are highly positive for pluripotency protein markers OCT-4 and SSEA-4, similar to that of the control group of fresh hiPSCs (Fig. 4A). Flow cytometry analyses are used to quantitatively evaluate the expression of pluripotency markers OCT-4 and SSEA-4. As shown in Fig. 4B–C, the cryopreserved hiPSCs highly express the two protein markers OCT-4 (96.7 ± 2.3%) and SSEA-4 (96.1 ± 1.6%), similar to the control fresh hiPSCs (97.2 ± 1.4% positive for OCT-4 and 98.0 ± 1.0% positive for SSEA-4) with no statistically significant difference. Moreover, the distribution of cryopreserved hiPSCs in the G1, S, and G2/M phases of cell cycle is similar to that of the control fresh cells (Fig. 4D–E) with no statistically significant difference. Hence, the cryopreserved hiPSCs have similar proliferation capacity as the control fresh cells. In other words, these data show that the cryopreservation procedure with sand-mediated ice seeding and 5% DMSO has no evident impact on the pluripotency/stemness/self-renewal and the proliferation capacity of the hiPSCs.

3.5. Intact capacity of differentiation of the cryopreserved hiPSCs

To ascertain their functional survival, the cryopreserved hiPSCs are further assessed for their capacity of guided neural and cardiac differentiation *in vitro* and spontaneous teratoma formation *in vivo*. After 10 days of neural differentiation, the cryopreserved hiPSCs lose their typical colony morphology and neurites are observable to extend out of the differentiated cells (Fig. 5A), similar to the fresh control cells (Fig. S3A). Furthermore, the resultant cells are positive for neural specific marker TUJ-1: 95.9 ± 1.5% of the cryopreserved hiPSCs post neural differentiation are positive for TUJ-1, similar to that (94.7 ± 2.5%) of the fresh control hiPSCs (Fig. S3B). These data demonstrate the cryopreserved hiPSCs maintain their capacity of neural differentiation. The capability of cardiac differentiation of the cryopreserved hiPSCs is also

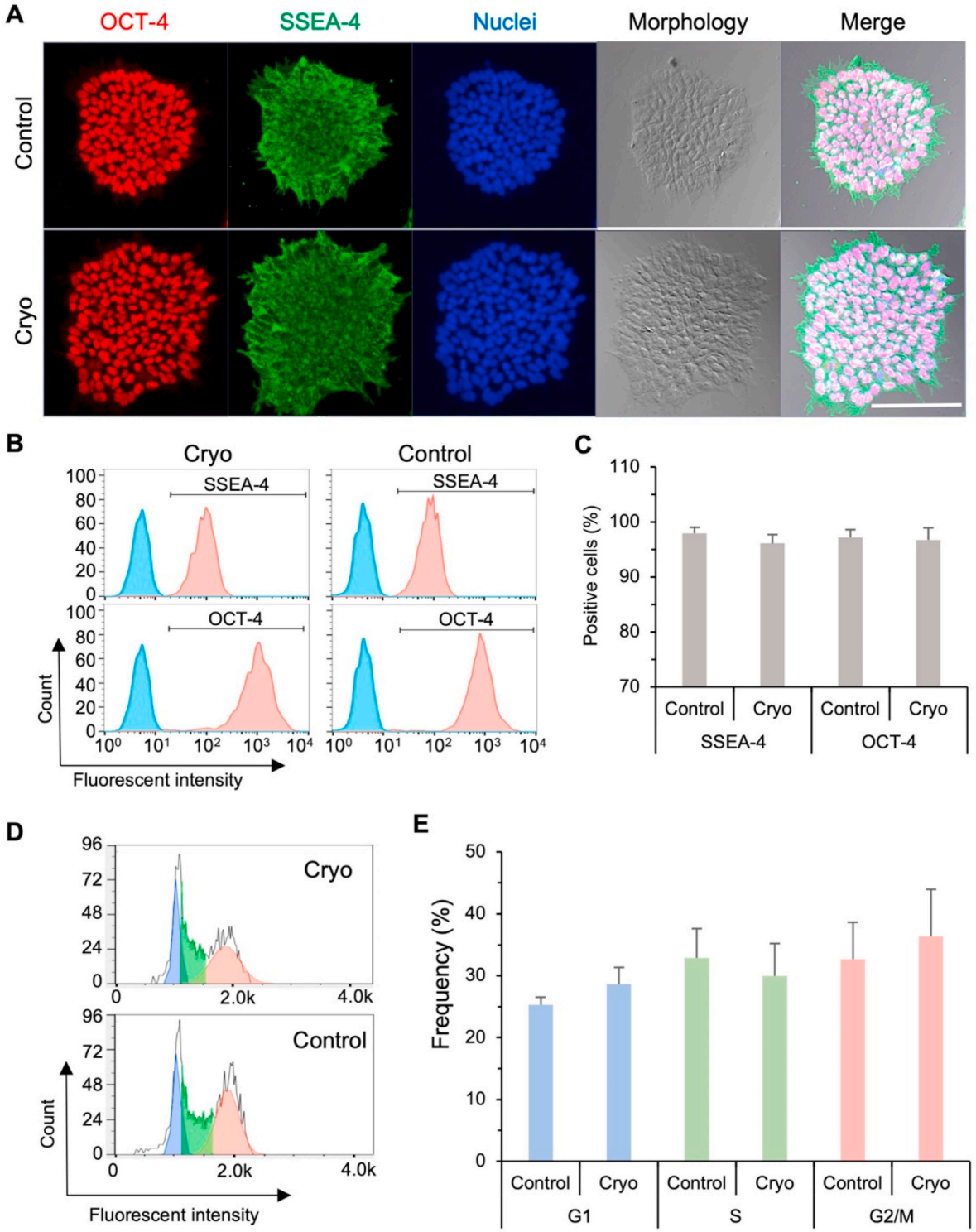

Fig. 4. Cryopreservation with sand-mediated ice seeding and 5% DMSO does not significantly affect the hiPSC pluripotency and cell cycle. (A) Images of cryopreserved (Cryo) hiPSCs showing typical colony morphology and high expression of pluripotency protein markers OCT-4 and SSEA-4, similar to fresh (Control) hiPSCs with no cryopreservation. Scale bar: 100 μm. (B–C) Representative peaks (B) and quantitative data (C, $n = 3$ independent runs) form flow cytometry analyses, showing the cryopreserved hiPSCs highly express pluripotency protein markers SSEA-4 and OCT-4 similar to the fresh control hiPSCs with no statistically significant difference. The light blue peaks are isotype controls. (D–E) Representative peaks (D) and quantitative data (E, $n = 3$ independent runs) from flow cytometry analyses, showing no statistically significant difference in the cell cycle distribution between the cryopreserved and fresh control hiPSCs.

evidenced by the spontaneously beating areas observable in 10 days after initiation of the differentiation (Movie S2), similar to the areas seen in the fresh control cells (Movie S3). The percentage of cells on day 10 positive for the cardiac specific marker cTnT is not significantly different between the cryo (87.9 ± 2.6%) and fresh control (85.6 ± 4.8%) groups (Fig. 5B). The cardiac muscle-like striated pattern can be seen on both the cTnT-stained fluorescence images and the non-fluorescence images showing the cell morphology of both cryopreserved (Fig. 5B) and fresh control (Figs. S3A and C) hiPSCs-derived cardiomyocytes. Lastly, the cryopreserved hiPSCs maintain the capability of teratoma formation *in*

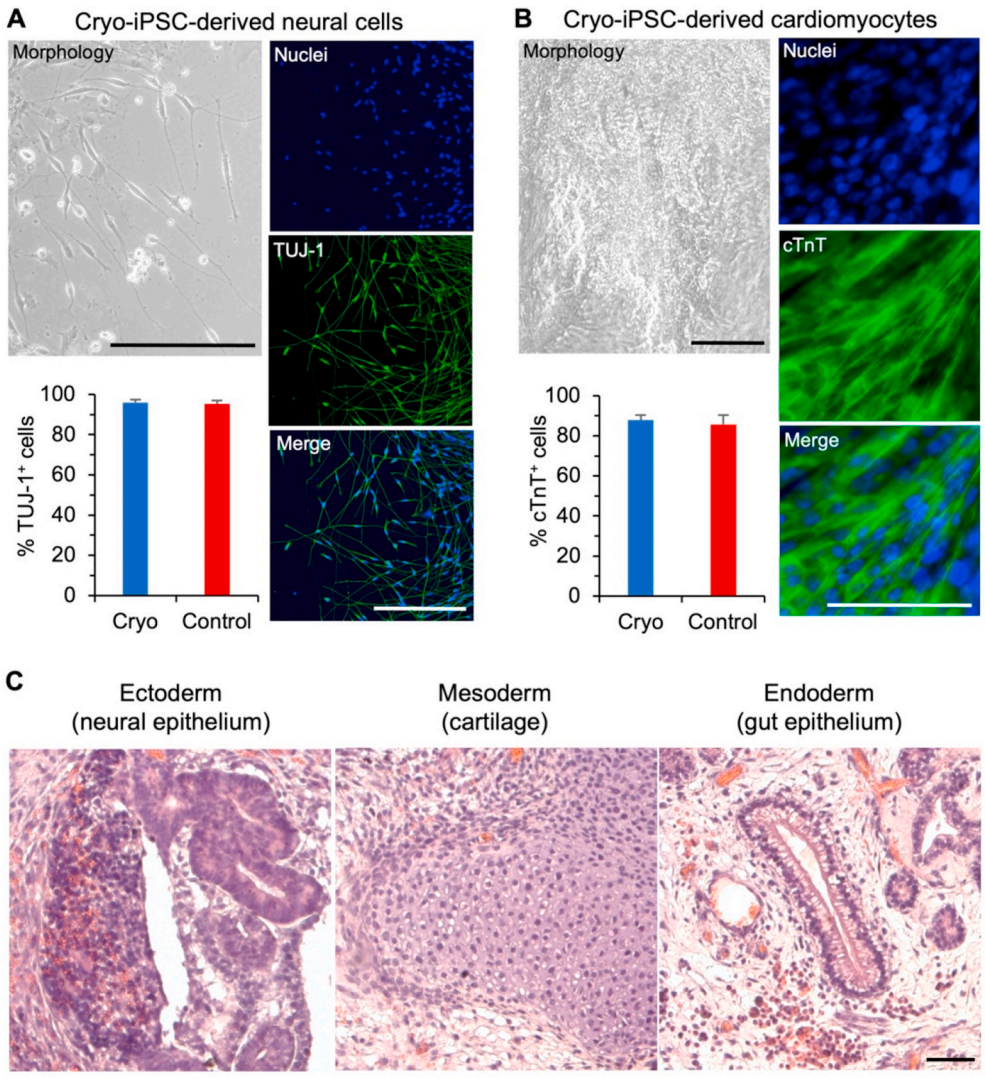

Fig. 5. Cryopreservation with sand-mediated ice seeding and 5% DMSO does not significantly affect the differentiation capacity of the hiPSCs. (A) The cryopreserved hiPSCs can efficiently differentiate into cells with typical neural cell morphology (neurites extending out of the cell body) and high expression of the neural specific marker TUJ-1. Cell nuclei are made visible by DAPI staining. (B) The cryopreserved hiPSCs can efficiently differentiate into cells that highly express the cardiac specific markers cTnT. Cell nuclei are made visible by DAPI staining. (C) The teratomas grown from the cryopreserved hiPSCs contain tissues from all the three germ layers including ectoderm (neural epithelium with hypernucelated neuroectodermal structures), mesoderm (the nidus of cartilage with surrounding condensed mesenchymal cells), and endoderm (gut epithelium with subnuclear vacuoles and tube-like structure). Scale bars: 100 μm.

vivo. The teratomas (Fig. 5C) grown from the cryopreserved hiPSCs show typical tissue structure of the three germ layers [44,45]: the neural epithelium of ectoderm with hypernucelated neuroectodermal structures, cartilage of mesoderm showing the nidus of cartilage with surrounding condensed mesenchymal cells, and gut epithelium of endoderm with subnuclear vacuoles and tube-like structure. Similar tissue structures are observable in the teratomas of the fresh control group (Fig. S3D). All these data on neural and cardiac differentiation *in vitro* and teratoma formation *in vivo* for the cryopreserved hiPSCs are similar to that for the fresh hiPSCs with no cryopreservation, showing cryopreservation with 5% DMSO and the sand-mediated ice seeding have no evident impact on the differentiation capacity of the hiPSCs.

4. Discussion

Human iPSCs can be derived from somatic cells like skin fibroblasts and blood cells of a specific person (patient or healthy donor) and have the capability of self-renewal and differentiation into somatic cells of all three germ-layers [46]. This eliminates the ethical concern of using embryonic stem cells. However, culturing hiPSCs at 37 °C is costly and their pluripotency and differentiation capability may decrease gradually over time during culture. Therefore, the quality of hiPSCs may be greatly compromised over long-term culture at 37 °C. As a result, efficient and convenient cryopreservation of hiPSCs to bank them in a state of "suspended animation" for their use at a desired future time is an enabling technology of the burgeoning hiPSC-based personalized medicine. However, the use of high concentrations of DMSO and serum in contemporary hiPSC cryopreservation protocols poses risks for the clinical use of the cryopreserved hiPSCs.

Current cryopreservation of hiPSCs utilizes two methods: vitrification and slow-freezing [47]. Although there is a higher survival for hiPSCs using vitrification than slow-freezing [48], vitrification requires high cooling rates achieved by specialized protocols/devices and/or high concentration of toxic CPA, making it difficult to scale-up for high-volume cell banking [49]. Slow-freezing is more convenient and widely used for cryopreservation of hiPSCs, with survival/recovery rates of ~50% [49–51]. This is similar to our control group (conventional method) shown in Fig. 3. Cryopreservation of hiPSCs is notably more difficult than cryopreservation of human adult stem cells (e.g., tissue-derived stem cells). Adult stem cells can be cryopreserved as single cells by traditional slow-freezing protocols with post-thaw viability up to 90% [52,53]. However, hiPSCs are more sensitive to stresses during cell cryopreservation, as hiPSCs grow in colonies with cell-cell and cell-matrix interactions and may undergo anoikis-induced apoptosis when dissociated into single cells. Therefore, hiPSCs are usually cryopreserved as small clumps supplemented with RI and serum to enhance their survival [54]. Neither RI nor serum is needed by our method for cryopreserving hiPSCs with sand-mediated ice seeding to achieve ~90% cell viability.

It is worth noting that we did not remove DMSO from the sample

immediately after thawing. This avoids centrifuging and rinsing the hiPSCs that just suffer the stresses during thawing and may be susceptible to the stresses associated with centrifugation and washing for removing DMSO immediately after thawing. However, the 250 μL of cryopreserved sample with hiPSCs was transferred into 2 mL of medium immediately thawing and the 5% DMSO was diluted to 0.56%. Moreover, the DMSO-containing medium was replaced with DMSO-free medium after only 2 h of incubation at 37 °C for the cells to recover. This low DMSO concentration and short incubation time should be safe for cells, as shown by the high viability of the cells cryopreserved using 5% DMSO with sand-mediated ice seeding (Fig. 3). This is not surprising because most of chemicals used for hiPSC maintenance are dissolved in DMSO with a final concentration up to 0.6% in the maintenance medium for the hiPSCs [55,56].

In this study, we used a natural and cost-effective material, sand, to seed/nucleate ice at high subzero temperature during cooling hiPSCs for cryopreservation with good outcome and reproducibility. The sands used in this study did not require any material or surface modification in order to achieve ice nucleation, making them convenient and cost-effective to use. This allows serum-free cryopreservation of hiPSCs with high viability and quality at a much reduced (half) DMSO concentration. The ice-seeding temperature of water containing the sand-PDMS film is significantly higher than that of water containing a pure PDMS film with no sand, which indicates that the sand plays an important role in seeding ice in water. This is consistent with the literature that quartz along with a few other minerals can seed ice in the atmosphere [57–59], because sands consist mainly of crystalline silica (silicon dioxide) that is also the material in quartz.

To further understand the role that the characteristics of sand played in inducing ice nucleation, specifically surface roughness/sharpness and surface composition (silicon dioxide) that determines the surface properties including hydrophobicity, the effects on ice-seeding temperature of plastic shard-PDMS film and glass bead-PDMS film were investigated. The glass beads are made of silicon dioxide (as with sands) with a smooth surface (Fig. S4A), which is studied to understand the effect of surface roughness/sharpness on ice seeding. The plastic shards have sharp edge as with sands (Fig. S4A) but a different composition from sands, which is examined to understand the effect of composition that determines the surface property including hydrophobicity (sand is more hydrophilic than the plastic shards) on ice seeding. The glass bead-PDMS film can improve the ice seeding-temperature significantly to -12.3 ± 1.8 °C from -15.9 ± 1.6 °C for water without anything for ice seeding (Figs. S4B–C). However, it is significantly lower than the ice-seeding temperature (-7.8 ± 1.6 °C) for the sand-PDMS film. This indicates both the silicon dioxide material and surface roughness/sharpness are important for ice seeding. The ice-seeding temperature for the plastic shard-PDMS film is -14.2 ± 1.1 °C (Figs. S4B–C), which is also significantly higher than that for control (i.e., water without anything for ice seeding) and significantly lower than that (-7.8 ± 1.6 °C) for sand-PDMS film. This further confirms the surface composition (that determines the surface property including hydrophobicity) is important for ice seeding. Collectively, these data indicate that both the surface composition (silicon dioxide) and roughness/sharpness render sands the excellent ice-seeding capability. In addition, the ice-seeding temperature for plastic shard-PDMS film is not significantly different from that (-14.9 ± 2.0 °C) of pure PDMS film while the ice-seeding temperature for glass bead-PDMS film is significantly higher than that of pure PDMS film, suggesting that the surface roughness/sharpness may be secondary to the surface composition (although both are important and might work synergistically) in determining the ice-seeding temperature.

Our studies show that controlled ice nucleation catalyzed by the sands greatly improves hiPSC survival post cryopreservation, from 52.6 ± 3.5% (5% DMSO, no ice seeding) to 90.3 ± 2.5% (5% DMSO, with ice seeding). This increase in survival is similar to other studies regarding the impact of controlled ice nucleation on cell survival using a slow-freezing protocol [27]. Other types of cells susceptible to freezing-induced stresses show a 15–40% increase in survival post-cryopreservation with ice nucleation versus without [27].

Of note, various methods have been explored to improve cryopreservation outcome including microencapsulation of cells in alginate hydrogel [23,60], nano-warming with magnetic nanoparticles [61–64], supplement of nontoxic CPAs like sugars into the cryopreservation medium [65–68], and intracellular delivery of the sugars using cold-responsive nanoparticles [53]. All these methods may be combined with our sand-mediated ice seeding, which has the potential to further reduce or even eliminate the DMSO needed for cryopreservation of the hiPSCs with high functional survival. Lastly, the method developed in this study may be applied to cryopreserve the iPSCs of non-human endangered species with high functional survival, which is valuable for animal species conservation [69].

5. Conclusion

We developed a novel method which uses sand as the ice-seeding material for cryopreservation of hiPSCs, resulting in ~90% hiPSC viability post-cryopreservation. The cryopreserved hiPSCs can attach well and maintain high pluripotency and differentiation capacity *in vitro* and *in vivo*. This method is simple to use, cost effective, and eliminates or reduces potentially clinically concerning elements in the cryopreservation solution. The sand mediated ice-seeding method has the potential to be widely used for cryopreservation of hiPSCs and potentially many other types of human cells for their ready availability to facilitate the widespread application of the burgeoning cell-based medicine and for cryopreservation of iPSCs of endangered species to promote animal species conservation.

CRediT author contribution statement

Bin Jiang: Conceptualization, Methodology, Investigation, Writing – original draft, Formal analysis. **Weijie Li:** Conceptualization, Methodology, Investigation, Writing – original draft, Formal analysis. **Samantha Stewart:** Methodology, Investigation, Writing – original draft, Formal analysis. **Wenquan Ou:** Investigation, Methodology, Formal analysis. **Baolin Liu:** Editing – original draft, Formal analysis. **Pierre Comizzoli:** Editing – original draft, Formal analysis. **Xiaoming He:** Conceptualization, Methodology, Resources, Writing – original draft, Formal analysis, Supervision, Project administration.

Declaration of competing interest

The authors declare that they have no known competing financial interests or personal relationships that could have appeared to influence the work reported in this paper.

Acknowledgments

This work was partially supported by grants from the US National Science Foundation (CBET-1831019 to XH and DGE-1840340 that is a GRFP fellowship to SS) and National Institutes of Health (NIH R01EB023632 to XH).

Appendix A. Supplementary data

Supplementary data to this article can be found online at https://doi.org/10.1016/j.bioactmat.2021.04.025.

References

[1] J. Yu, M.A. Vodyanik, K. Smuga-Otto, J. Antosiewicz-Bourget, J.L. Frane, S. Tian, J. Nie, G.A. Jonsdottir, V. Ruotti, R. Stewart, I.I. Slukvin, J.A. Thomson, Induced pluripotent stem cell lines derived from human somatic cells, Science 318 (5858) (2007) 1917–1920.

[2] V.K. Singh, M. Kalsan, N. Kumar, A. Saini, R. Chandra, Induced pluripotent stem cells: applications in regenerative medicine, disease modeling, and drug discovery, Frontiers in Cell and Developmental Biology 3 (2015).

[3] J. Wang, J. Hao, D. Bai, Q. Gu, W. Han, L. Wang, Y. Tan, X. Li, K. Xue, P. Han, Z. Liu, Y. Jia, J. Wu, L. Liu, L. Wang, W. Li, Z. Liu, Q. Zhou, Generation of clinical-grade human induced pluripotent stem cells in Xeno-free conditions, Stem Cell Res. Ther. 6 (1) (2015).

[4] C.-Y. Huang, C.-L. Liu, C.-Y. Ting, Y.-T. Chiu, Y.-C. Cheng, M.W. Nicholson, P.C. H. Hsieh, Human iPSC banking: barriers and opportunities, J. Biomed. Sci. 26 (1) (2019).

[5] B. Jiang, L. Yan, J.G. Shamul, M. Hakun, X. He, Stem cell therapy of myocardial infarction: a promising opportunity in bioengineering, Advanced Therapeutics 3 (2020), 1900182.

[6] Y. Xu, C. Chen, P.B. Hellwarth, X. Bao, Biomaterials for stem cell engineering and biomanufacturing, Bioact Mater 4 (2019) 366–379.

[7] I. Massie, C. Selden, H. Hodgson, B. Fuller, S. Gibbons, G.J. Morris, GMP cryopreservation of large volumes of cells for regenerative medicine: active control of the freezing process, Tissue Eng. C Methods 20 (9) (2014) 693–702.

[8] V. Stensvaag, T. Furmanek, K. Lønning, A.J.A. Terzis, R. Bjerkvig, T. Visted, Cryopreservation of alginate-encapsulated recombinant cells for antiangiogenic therapy, Cell Transplant. 13 (1) (2004) 35–44.

[9] V. Isachenko, E. Isachenko, J. Reinsberg, M. Montag, F. Braun, H. Van Der Ven, Cryopreservation of human ovarian tissue: effect of spontaneous and initiated ice formation, Reprod. Biomed. Online 16 (3) (2008) 336–345.

[10] Y. Yuan, Y. Yang, Y. Tian, J. Park, A. Dai, R.M. Roberts, Y. Liu, X. Han, Efficient long-term cryopreservation of pluripotent stem cells at -80 degrees C, Sci. Rep. 6 (2016) 34476.

[11] M.A. Cox, J. Kastrup, M. Hrubiško, Historical perspectives and the future of adverse reactions associated with haemopoietic stem cells cryopreserved with dimethyl sulfoxide, Cell Tissue Bank. 13 (2) (2012) 203–215.

[12] S. Rowley, G. Anderson, Effect of DMSO exposure without cryopreservation on hematopoietic progenitor cells, Bone Marrow Transplant. 11 (5) (1993) 389–393.

[13] L. Weng, P.R. Beauchesne, Dimethyl sulfoxide-free cryopreservation for cell therapy: a review, Cryobiology 94 (2020) 9–17.

[14] C. Bueno, R. Montes, P. Menendez, The ROCK inhibitor Y-27632 negatively affects the expansion/survival of both fresh and cryopreserved cord blood-derived CD34+ hematopoietic progenitor cells, Stem Cell Reviews and Reports 6 (2010) 215–223.

[15] S. Chetty, F.W. Pagliuca, C. Honore, A. Kweudjeu, A. Rezania, D.A. Melton, A simple tool to improve pluripotent stem cell differentiation, Nat. Methods 10 (6) (2013) 553–556.

[16] M. Verheijen, M. Lienhard, Y. Schrooders, O. Clayton, R. Nudischer, S. Boerno, B. Timmermann, N. Selevsek, R. Schlapbach, H. Gmuender, S. Gotta, J. Geraedts, R. Herwig, J. Kleinjans, F. Caiment, DMSO induces drastic changes in human cellular processes and epigenetic landscape in vitro, Sci. Rep. 9 (1) (2019).

[17] T.A. Grein, D. Freimark, C. Weber, K. Hudel, C. Wallrapp, P. Czermak, Alternatives to dimethylsulfoxide for serum-free cryopreservation of human mesenchymal stem cells, Int. J. Artif. Organs 33 (6) (2010) 370–380.

[18] J. Seremak, A. Eroglu, Chemically defined and xeno-free cryopreservation of human-induced pluripotent stem cells, Methods Mol. Biol. 2180 (2021) 569–579.

[19] P. Mazur, Freezing of living cells: mechanisms and implications, Am. J. Physiol. Cell Physiol. 247 (3) (1984) C125–C142.

[20] F.W. Kleinhans, Membrane permeability modeling: Kedem–Katchalsky vs a two-parameter formalism, Cryobiology 37 (4) (1998) 271–289.

[21] K.R. Diller, Quantitative low temperature optical microscopy of biological systems, J. Microsc. 126 (Pt 1) (1982) 9–28.

[22] F. Franks, biophysics and biochemistry at low temperatures, FEBS Lett. 220 (1) (1987).

[23] H. Huang, J.K. Choi, W. Rao, S. Zhao, P. Agarwal, G. Zhao, X. He, Alginate hydrogel microencapsulation inhibits devitrification and enables large-volume low-CPA cell vitrification, Adv. Funct. Mater. 25 (2015) 6839–6850.

[24] X. He, J.C. Bischof, Quantification of temperature and injury response in thermal therapy and cryosurgery, Crit. Rev. Biomed. Eng. 31 (5–6) (2003) 355–422.

[25] X. He, Thermostability of biological systems: fundamentals, challenges, and quantification, Open Biomed. Eng. J. 5 (2011) 47–73.

[26] H. Huang, G. Zhao, Y. Zhang, J. Xu, T.L. Toth, X. He, Predehydration and ice seeding in the presence of trehalose enable cell cryopreservation, ACS Biomater. Sci. Eng. 3 (8) (2017) 1758–1768.

[27] G.J. Morris, E. Acton, Controlled ice nucleation in cryopreservation–a review, Cryobiology 66 (2) (2013) 85–92.

[28] P.M. Zavos, E.F. Graham, Effects of various degrees of supercooling and nucleation temperatures on fertility of frozen Turkey spermatozoa, Cryobiology 20 (5) (1983) 553–559.

[29] P. Mazur, Physical and temporal factors involved in the death of yeast at subzero temperatures, Biophys. J. 1 (3) (1961) 247–264.

[30] F.S. Trad, M. Toner, J.D. Biggers, Effects of cryoprotectants and ice-seeding temperature on intracellular freezing and survival of human oocytes, Hum. Reprod. 14 (6) (1999) 1569–1577.

[31] C.E. Morris, D.G. Georgakopoulos, D.C. Sands, Ice nucleation active bacteria and their potential role in precipitation, J. Phys. IV 121 (2004) 87–103.

[32] L.R. Maki, E.L. Galyan, M.-M. Chang-Chien, D.R. Caldwell, Ice nucleation induced by *Pseudomonas syringae*, Appl. Microbiol. 28 (3) (1974) 456–459.

[33] F.W. Kleinhans, J.F. Guenther, D.M. Roberts, P. Mazur, Analysis of intracellular ice nucleation in Xenopus oocytes by differential scanning calorimetry, Cryobiology 52 (1) (2006) 128–138.

[34] B. Jin, S. Seki, E. Paredes, J. Qiu, Y. Shi, Z. Zhang, C. Ma, S. Jiang, J. Li, F. Yuan, S. Wang, X. Shao, P. Mazur, Intracellular ice formation in mouse zygotes and early morulae vs. cooling rate and temperature-experimental vs. theory, Cryobiology 73 (2) (2016) 181–186.

[35] I. Massie, C. Selden, H. Hodgson, B. Fuller, Cryopreservation of encapsulated liver spheroids for a bioartificial liver: reducing latent cryoinjury using an ice nucleating agent, Tissue Eng. C Methods 17 (7) (2011) 765–774.

[36] T. Kojima, T. Soma, N. Oguri, Effect of ice nucleation by droplet of immobilized silver iodide on freezing of rabbit and bovine embryos, Theriogenology 30 (6) (1988) 199–1207.

[37] T. Kojima, T. Soma, N. Oguri, Effect of silver iodide as an ice inducer on viability of frozen-thawed rabbit morulae, Theriogenology 26 (3) (1986) 341–352.

[38] W. Rao, H. Huang, H. Wang, S. Zhao, J. Dumbleton, G. Zhao, X. He, Nanoparticle-mediated intracellular delivery enables cryopreservation of human adipose-derived stem cells using trehalose as the sole cryoprotectant, ACS Appl. Mater. Interfaces 7 (2015) 5017–5028.

[39] A. Morizane, D. Doi, T. Kikuchi, K. Nishimura, J. Takahashi, Small-molecule inhibitors of bone morphogenic protein and activin/nodal signals promote highly efficient neural induction from human pluripotent stem cells, J. Neurosci. Res. 89 (2) (2011) 117–126.

[40] G. Lee, S.M. Chambers, M.J. Tomishima, L. Studer, Derivation of neural crest cells from human pluripotent stem cells, Nat. Protoc. 5 (4) (2010) 688–701.

[41] S.M. Chambers, C.A. Fasano, E.P. Papapetrou, M. Tomishima, M. Sadelain, L. Studer, Highly efficient neural conversion of human ES and iPS cells by dual inhibition of SMAD signaling, Nat. Biotechnol. 27 (3) (2009) 275–280.

[42] B. Jiang, Z. Xiang, Z. Ai, H. Wang, Y. Li, W. Ji, T. Li, Generation of cardiac spheres from primate pluripotent stem cells in a small molecule-based 3D system, Biomaterials 65 (2015) 103–114.

[43] T.G. Otsuji, J. Bin, A. Yoshimura, M. Tomura, D. Tateyama, I. Minami, Y. Yoshikawa, K. Aiba, J.E. Heuser, T. Nishino, K. Hasegawa, N. Nakatsuji, A 3D sphere culture system containing functional polymers for large-scale human pluripotent stem cell production, Stem cell reports 2 (5) (2014) 746.

[44] I. Damjanov, P.W. Andrews, Teratomas produced from human pluripotent stem cells xenografted into immunodeficient mice - a histopathology atlas, Int. J. Dev. Biol. 60 (10–11-12) (2016) 337–419.

[45] H. Hentze, P.L. Soong, S.T. Wang, B.W. Phillips, T.C. Putti, N.R. Dunn, Teratoma formation by human embryonic stem cells: evaluation of essential parameters for future safety studies, Stem Cell Res. 2 (3) (2009) 198–210.

[46] Y. Jiang, X.L. Lian, Heart regeneration with human pluripotent stem cells: prospects and challenges, Bioact Mater 5 (1) (2020) 74–81.

[47] C.J. Hunt, Technical considerations in the freezing, low-temperature storage and thawing of stem cells for cellular therapies, Transfus. Med. Hemotherapy 46 (3) (2019) 134–150.

[48] Y. Li, J.C. Tan, L.S. Li, Comparison of three methods for cryopreservation of human embryonic stem cells, Fertil. Steril. 93 (3) (2010) 999–1005.

[49] Y. Miyamoto, H. Noguchi, H. Yukawa, K. Oishi, K. Matsushita, H. Iwata, S. Hayashi, Cryopreservation of induced pluripotent stem cells, Cell Med. 3 (1–3) (2012) 89–95.

[50] W. Liu, G. Chen, Cryopreservation of human pluripotent stem cells in defined medium, Curr Protoc Stem Cell Biol 31 (2014) 1C 17 1–13.

[51] K. Imaizumi, N. Nishishita, M. Muramatsu, T. Yamamoto, C. Takenaka, S. Kawamata, K. Kobayashi, S. Nishikawa, T. Akuta, A simple and highly effective method for slow-freezing human pluripotent stem cells using dimethyl sulfoxide, hydroxyethyl starch and ethylene glycol, PloS One 9 (2) (2014), e88696.

[52] G. Zhao, X. Liu, K. Zhu, X. He, Hydrogel encapsulation facilitates rapid-cooling cryopreservation of stem cell-Laden core-shell microcapsules as cell-biomaterial constructs, Advanced healthcare materials 6 (23) (2017).

[53] Y. Zhang, H. Wang, S. Stewart, B. Jiang, W. Ou, G. Zhao, X. He, Cold-responsive nanoparticle enables intracellular delivery and rapid release of trehalose for organic-solvent-free cryopreservation, Nano Lett. 19 (12) (2019) 9051–9061.

[54] T. Miyazaki, H. Suemori, Slow cooling cryopreservation optimized to human pluripotent stem cells, Adv. Exp. Med. Biol. 951 (2016) 57–65.

[55] T.W. Theunissen, B.E. Powell, H. Wang, M. Mitalipova, D.A. Faddah, J. Reddy, Z. P. Fan, D. Maetzel, K. Ganz, L. Shi, T. Lungjangwa, S. Imsoonthornruksa, Y. Stelzer, S. Rangarajan, A. D'Alessio, J. Zhang, Q. Gao, M.M. Dawlaty, R.A. Young, N. S. Gray, R. Jaenisch, Systematic identification of culture conditions for induction and maintenance of naive human pluripotency, Cell Stem Cell 15 (4) (2014) 471–487.

[56] S. Chetty, F.W. Pagliuca, C. Honore, A. Kweudjeu, A. Rezania, D.A. Melton, A simple tool to improve pluripotent stem cell differentiation, Nat. Methods 10 (6) (2013) 553–556.

[57] A. Kumar, C. Marcolli, T. Peter, Ice nucleation activity of silicates and aluminosilicates in pure water and aqueous solutions – Part 2: quartz and amorphous silica, Atmos. Chem. Phys. 19 (9) (2019) 6035–6058.

[58] A.D. Harrison, K. Lever, A. Sanchez-Marroquin, M.A. Holden, T.F. Whale, M. D. Tarn, J.B. Mcquaid, B.J. Murray, The ice-nucleating ability of quartz immersed in water and its atmospheric importance compared to K-feldspar, Atmos. Chem. Phys. 19 (17) (2019) 11343–11361.

[59] M.A. Holden, T.F. Whale, M.D. Tarn, D. O'Sullivan, R.D. Walshaw, B.J. Murray, F. C. Meldrum, H.K. Christenson, High-speed imaging of ice nucleation in water proves the existence of active sites, Science Advances 5 (2) (2019), eaav4316.

[60] W. Zhang, G. Yang, A. Zhang, L.X. Xu, X. He, Preferential vitrification of water in small alginate microcapsules significantly augments cell cryopreservation by vitrification, Biomed. Microdevices 12 (1) (2010) 89–96.

[61] J. Wang, G. Zhao, Z. Zhang, X. Xu, X. He, Magnetic induction heating of superparamagnetic nanoparticles during rewarming augments the recovery of hUCM-MSCs cryopreserved by vitrification, Acta Biomater. 33 (2016) 264–274.

[62] N. Manuchehrabadi, Z. Gao, J. Zhang, H.L. Ring, Q. Shao, F. Liu, M. McDermott, A. Fok, Y. Rabin, K.G.M. Brockbank, M. Garwood, C.L. Haynes, J.C. Bischof, Improved tissue cryopreservation using inductive heating of magnetic nanoparticles, Sci. Transl. Med. 9 (379) (2017), eaah4586.
[63] X. Liu, G. Zhao, Z. Chen, F. Panhwar, X. He, Dual suppression effect of magnetic induction heating and microencapsulation on ice crystallization enables low-cryoprotectant vitrification of stem cell-alginate hydrogel constructs, ACS Appl. Mater. Interfaces 10 (19) (2018) 16822–16835.
[64] Y. Cao, G. Zhao, F. Panhwar, X. Zhang, Z. Chen, L. Cheng, C. Zang, F. Liu, Y. Zhao, X. He, The unusual properties of polytetrafluoroethylene enable massive-volume vitrification of stem cells with low-concentration cryoprotectants, Adv Mater Technol 4 (1) (2019) 1800289.
[65] S. Stewart, X. He, Intracellular delivery of trehalose for cell banking, Langmuir 35 (23) (2019) 7414–7422.
[66] J.H. Crowe, L.M. Crowe, Preservation of mammalian cells-learning nature's tricks, Nat. Biotechnol. 18 (2) (2000) 145–146.
[67] C. Gläfke, M. Akhoondi, H. Oldenhof, H. Sieme, W.F. Wolkers, Cryopreservation of platelets using trehalose: the role of membrane phase behavior during freezing, Biotechnol. Prog. 28 (5) (2012) 1347–1354.
[68] A. Eroglu, M.J. Russo, R. Bieganski, A. Fowler, S. Cheley, H. Bayley, M. Toner, Intracellular trehalose improves the survival of cryopreserved mammalian cells, Nat. Biotechnol. 18 (2) (2000) 163–167.
[69] G.F. Mastromonaco, L.A. Gonzalez-Grajales, M. Filice, P. Comizzoli, Somatic cells, stem cells, and induced pluripotent stem cells: how do they now contribute to conservation? Adv. Exp. Med. Biol. 753 (2014) 385–427.